Journal of Geomine (2025), 3(1), 70-81
DOI: 10.22077/jgm.2025.9258.1045

Geoelectrical modeling of time-domain electrical resistivity and induced polarization data for imaging marble building stone

Seyed Mohammad Mehdi Hosseini Asil[1], Maysam Abedi[1], Ali Moradzadeh[1]

Recived: 2025 Apr. 20, Revised: 2025 Jul. 28, Online Published: 2025 Aug. 04

ABSTRACT

Integrated geoelectrical data modeling aims to produce subsurface electrical models for mineral deposit exploration. These models improve understanding of subsurface lithology and structures. Quantitative interpretation using numerical inversion is crucial for accurate results. This study employs 2D inversion of time-domain electrical resistivity and induced polarization data from three profiles to investigate marble deposits in Iran's Fasa region. This research aims to identify and differentiate the bedrock from the marble deposit. The methods used in this study include electrical resistivity tomography through dipole-dipole and pole-dipole configurations. Based on the obtained results, the separation of the marble stone from the background is illustrated using electrical characteristics. Additionally, the boundaries and the greater continuity of the building stone mass are also discussed. The thickness of the marble layer was determined to range between 10 and 30 meters, In comparison, the surface sandstone/limestone layer displayed thickness variations from zero up to 30 meters, characterized by notably lower electrical resistivity. Furthermore, the induced polarization models revealed the existence of a limestone/marl bed containing marble at depths ranging from 30 to 40 meters. Additionally, the electrical resistivity models indicated that the marble layer located in the southern region is of superior quality compared to that found in the mountain ridge. In the modeling, an attempt has been made to minimize the difference between the observed and predicted apparent values, and accordingly, the RMS error rate was less than 2.

KEYWORDS

Numerical modeling, Induced polarization, Electrical resistivity, Inversion, Marble stone

I. INTRODUCTION

Geophysical techniques are utilized to assess the physical characteristics of underground rock formations through instruments strategically positioned on the air, Earth's surface, borhole or under water. These assessments play a crucial role in identifying the presence of economically significant resources. Among diverse array of geophysical methodologies, electrical and electromagnetic surveys, are employed to map the electrical properties of the subsurface. These methodologies encompass both passive and active surveying approaches, each tailored to enhance our understanding of the hidden geological setting. In passive surveying techniques, the focus lies on the measurement of natural electric or electromagnetic (EM) fields, employing straightforward survey instruments that facilitate the process. Conversely, active surveying methods involve the deliberate transmission of an electrical signal into the subsurface, utilizing advanced multi-channel equipment to capture a variety of parameters that pertain to the electrical characteristics of subsurface phenomena (Abedi and Afshar, 2021; Dentith and Mudge, 2014). Electrical exploration focuses on identifying surface phenomena that arise from the flow of electric current through the Earth's subsurface. In contrast to other exploration techniques like gravity, magnetometry, seismic analysis, and radioactivity, electrical methods present a more diverse range of applications. This versatility allows for a more comprehensive understanding of geological structures and conditions, enhancing the effectiveness of exploration efforts. Time domain Electrical Resistivity Tomography (ERT) is among popular electrical surveys which provide helpful information about electrical resistivity and induced polarization (Binley and Kemna, 2005; Loke and Barker, 1996; Oldenburg and Li, 1999).

The techniques of electrical resistivity and induced polarization underwent significant refinement and found widespread application in recent decades. In the 1960s, the geophysical exploration landscape was

[1] School of Mining Engineering, College of Engineering, University of Tehran, Tehran, Iran
✉ M. Abedi: maysamabedi@ut.ac.ir

notably transformed by the adoption of time-domain and frequency-domain techniques. These methodologies quickly became favored during the 1960s and 1970s, particularly for the exploration of porphyry and massive sulfide deposits, as their effectiveness became increasingly recognized (Hoover et al., 1995; Sumner, 2012). Initially, the application of induced polarization and resistivity methods was hampered by computational and instrumental constraints, which limited their broader use (Dahlin, 1996; Telford et al., 1990).

Electromagnetic methods, particularly electrical resistivity and induced polarization techniques, have become indispensable tools in mineral exploration, geotechnical assessments, and environmental studies. These methods allow for the mapping of subsurface materials by measuring their electrical properties, which can indicate the presence of valuable minerals such as gold, copper, and lithium (Reynolds, 2011). Furthermore, in engineering geology, geoelectrical methods help identify soil and rock characteristics essential for construction projects (Loke and Barker,1996). In environmental assessments, they are employed to detect contamination and analyze groundwater flow (Dahlin, 1996). Notably, these methods have also seen success in the exploration of building stones, with studies demonstrating their effectiveness in delineating limestone and granite deposits (Keller and Frischknecht, 1966; Edigbue et al., 2021), showcasing their versatility and efficacy across various geological applications. In recent times, a variety of geophysical techniques have been harnessed to investigate valuable natural resources, with electrical resistivity, seismic refraction, and ground-penetrating radar (GPR) standing out as some of the most prevalent methods employed in the field (Annan and Jol, 2009; Ganiyu et al., 2020). GPR and ERT are adept at producing high-resolution images that play a crucial role in pinpointing fractured and weathered travertine deposits throughout the mining operations (Annan, 2003; Demirel et al., 2016; Kemna et al., 2005).

Several studies have extensively explored the application of geophysical and geoelectrical methods for the exploration and characterization of building stones. To investigate the travertine building stone formations in the Atashkooh region of Iran, comprehensive geoelectrical studies have been successfully executed. These studies involved the simultaneous analysis of electrical resistivity and chargeability data, allowing for a detailed understanding of the layering and geometry of the travertine based on its unique electrical characteristics (Talebi et al., 2022a, 2022b). Research has demonstrated the effectiveness of resistivity imaging in evaluating the characteristics of stone materials used in construction, as highlighted by Uhlemann et al. (2018). The combination of electrical resistivity and seismic data offers valuable insights into the geological factors that affect the quality of building stones, as noted by Cardarelli et al. (2010). Furthermore, Martinez et al. (2017) investigate the use of integrated geophysical techniques, such as magnetometry and electrical resistivity, to accurately identify and delineate marble mining areas, thereby enhancing extraction efficiency. In a separate study, Ahmed et al. (2023) assess non-destructive testing methods for granite, marble, and sandstone in North Pakistan, aiming to ensure reliable evaluations that facilitate effective resource management and quality control in stone extraction. Additionally, the suitability of weathered granite as a building material has been validated through electrical resistance assessments (Olona et al., 2010). Lastly, Jarzyna et al. (2012) explore various near-surface geophysical techniques for the exploration of limestone and granite, further underscoring the importance of these methods in evaluating construction materials.

Iran's strategic position along the orogenic belt, coupled with its rich geological history spanning multiple eras, has created an ideal setting for the development of a wide array of mineral resources since ancient times. Notably, the country boasts a remarkable abundance and variety of building and façade stones, earning it the distinction of being the eighth largest in this category on a global scale. As a result, Iran has established itself as the fourth-largest stone producer worldwide, trailing only behind industry giants such as China, India, and Italy (Abedi and Afshar, 2021Iran boasts a rich array of stone resources, which can be primarily classified into travertine, marble, onyx, and granite, showcasing the remarkable variety of reserves at hand. The distribution map of building stone mines in Iran, depicted in Fig.1, further emphasizes the geographical spread of these valuable resources.

This study has focused on a region in Fars Province, located about 180 kilometers southeast of Shiraz, specifically within the Sheshdeh district of Fasa County. Geologically, this area is part of the intricately folded Zagros belt, known for its tightly packed and compressed anticlines, which predominantly exhibit vertical axial planes oriented in a northwest-southeast direction. The research presents findings from geoelectrical investigations conducted along three carefully designed profiles, utilizing time-domain electrical resistivity (RS) and induced polarization (IP) measurements. The primary objective is to precisely determine the location, shape, and depth of marble layers while assessing their quality concerning fractures and fissures. Subsequently, the study will employ a 2D ERT inversion technique to evaluate the viability of extracting these marble deposits.

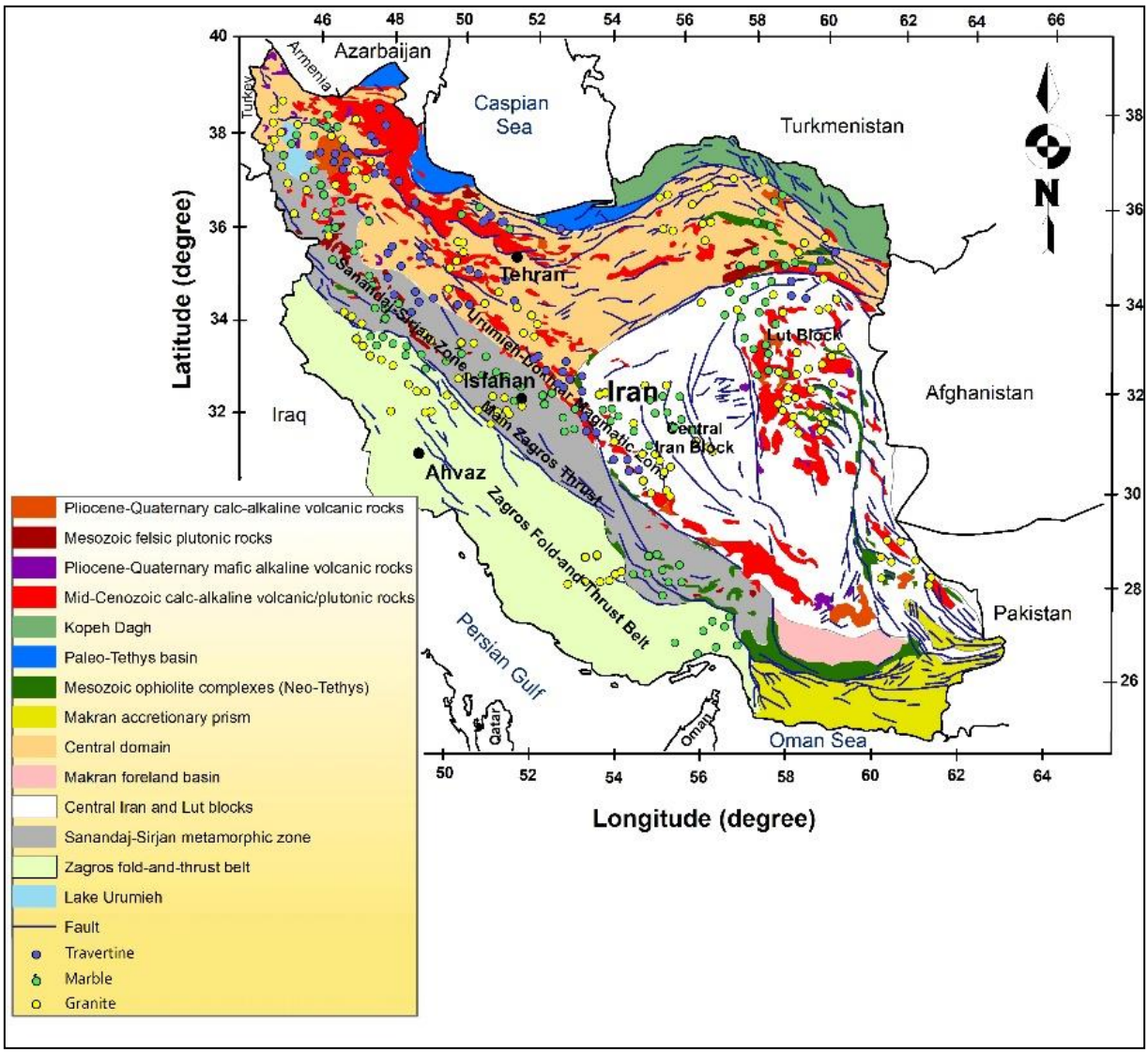

Fig. 1. Map of Building Stone Distribution over the structural geology map of Iran

II. RESEARCH METHODOLOGY

In the realm of geoelectrical investigations, the apparent resistivity and chargeability values obtained from measurements do not inherently yield a clear representation of the subsurface geoelectric characteristics. Consequently, the analysis of these measured data necessitates the use of inverse modeling techniques. Forward modeling is employed to simulate the resistivity and chargeability responses corresponding to a specified subsurface geoelectric model. In contrast, the inverse modeling works to reconstruct the geoelectric structure by interpreting the collected dataset. Historically, the analysis of 1D surveys, and occasionally 3D datasets, relied on manual curve-matching techniques that employed both primary and auxiliary curves to interpret precomputed responses from a variety of two- and three-layer models (Loke and Barker, 1996; Dey and Morrison, 1979). Such type of modeling cannot accurately represent the realastic geometry of subsurface targets. A contemporary method for data inversion entails leveraging information derived from forward models to identify a comprehensive resistivity distribution model that aligns most closely with the measured data (Rücker et al., 2006; Sharma and Verma, 2015).

A. Survey Configuration

To achieve an accurate representation of the Earth's subsurface, a quantitative interpretation is essential, necessitating the use of numerical modeling techniques. This study is specifically designed to distinguish between various regions characterized by differing electrical resistivity and chargeability, utilizing the data collected from geoelectrical surveys conducted throughout the area. The survey data was designed across three ERT profiles through a measurement system crafted by IRIS, a renowned French manufacturer. This electrical setup comprises a VIP 5000 current transmitter, paired with an ELREC10 receiver and a robust 5000-watt current generator. For

potential measurements, a 20-electrode cable configuration was employed, as illustrated in Fig. 2, which showcases the study area, survey lines, and the equipment utilized. Following the acquisition of data, inversion modeling was executed using the Res2DInv software, which involved the removal of noisy data points (Loke and Barker, 1996; Rücker et al., 2006). This well-known software employs an optimization method aimed at minimizing discrepancies between the observed and calculated values of apparent resistivity and polarization by fine-tuning the resistivity and polarization parameters of each block when discretizing the physical domain. The effectiveness of this process is ultimately assessed through the Root Mean Square (RMS) error factor. The fundamental approach in modeling with Res2DInv involves selecting an initial IP and RS model, ensuring that the RMS error values remain relatively stable throughout the iterative process. Furthermore, an algorithm was implemented to mitigate noise interference, facilitating the development of models characterized by optimal horizontal smoothing to retrieve better a layered marble target (Dey and Morrison, 1979; Sharma and Verma, 2015). In addition, a dipole-dipole array was employed to characterize the lateral variability of electrical properties in the subsurface layers, including potential marble lenses. Complementary pole-dipole measurements were acquired to probe deeper structures. This dual-array approach enables simultaneous investigation of both lateral heterogeneity and vertical depth penetration with enhanced resolution. The spacing of the electric dipoles was also determined by the estimated thickness of the marble layers and lenses within the study area.

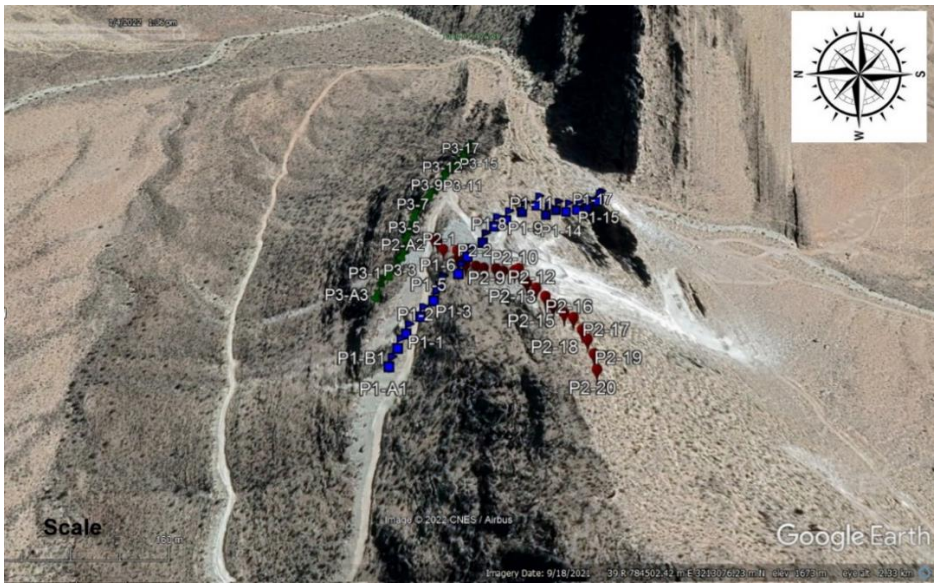

(a)

(b)

Fig. 2. View of the study area and survey lines (a), and depiction of the survey equipment (b).

B. ERT Data Inversion

The res2dinv software package has gained significant popularity in the field of geophysical surveys, particularly within Earth sciences, for its adeptness in inverting apparent ERT data to facilitate detailed subsurface mapping. This tool utilizes an array of mathematical models to conduct both forward and inversion modeling, thereby enhancing our comprehension of the electrical characteristics arising from geological formations. Its application is crucial for geoscientists seeking to discover the complexities of the Earth's subsurface, making it an indispensable asset in the geo-electric field. The inversion methodology implemented within the program is founded upon the principles of the smoothness-constrained least-squares method, as referenced in sources (Constable et al., 1987; Loke et al., 2014; Cardarelli and Fischanger, 2006). This approach is based on a specific mathematical equation that operates as follows:

$$(J^T J + uF)d = J^T g \quad (1)$$

Where, $F = f_x f_x^T + f_z f_z^T$, f_x is horizontal flatness filters, f_z presents vertical flatness filter, J shows a Jacobian matrix or kernel determined from partial derivatives, J^T is transpose of J, u indicates damping factor or regularization parameter for balancing data misfit or model norms, d is model perturbation vector. Finally g shows discrepancy vector between observed and predicted electrical data.

One notable benefit of this approach lies in its flexibility, allowing for the customization of the damping factor and roughness filters to accommodate various data types. For an in-depth exploration of the various adaptations of the smoothness-constrained least-squares method, one can refer to the complementary tutorial notes provided by Loke (2018).

The program introduces an innovative implementation of the least-squares method, leveraging a quasi-Newton optimization technique that significantly enhances performance (Loke and Barker, 1996). This advanced approach boasts a speed that surpasses the traditional least-squares method by over tenfold when handling extensive data sets, all while utilizing less memory. Additionally, users have the option to employ the classic Gauss-Newton method within the program. Although this method operates at a slower pace compared to its quasi-Newton counterpart, it tends to yield marginally superior results in scenarios characterized by substantial resistivity contrasts exceeding 10:1. Furthermore, the program offers a third alternative, allowing users to initiate the process with the Gauss-Newton method for the first two or three iterations before transitioning to the quasi-Newton method. This strategic combination often strikes an optimal balance, delivering impressive results across various applications (Reynolds, 2011).

The 2D model employed by this software intricately segments the subsurface into a series of rectangular blocks. This program's primary objective is to ascertain the electrical resistivity and chargeability of these blocks, thereby generating an apparent ERT pseudo-section that aligns closely with actual field measurements. For the Wenner and Schlumberger arrays, the initial layer's thickness is established at 0.5 times the distance between electrodes. In contrast, for the pole-pole, dipole-dipole, and pole-dipole arrays, the thicknesses are calibrated to approximately 0.9, 0.3, and 0.6 times the electrode spacing, respectively. Furthermore, the thickness of each subsequent layer, positioned at greater depths, is typically increased by 10% or 25%. Users also have the flexibility to manually adjust the depths of these layers to suit specific requirements.

The optimization technique aims to minimize the disparity between the computed and observed apparent ERT values by fine-tuning the resistivity and chargeability of the model blocks, all while adhering to established smoothness constraints. The RMS error serves as a quantifiable indicator of this discrepancy. Nevertheless, a model that achieves the lowest RMS error may exhibit significant and unrealistic fluctuations in model values, which may not necessarily represent the most accurate geological interpretation. Typically, the most judicious strategy is to select the model from the iteration where the RMS error stabilizes and shows minimal change. This phenomenon generally manifests during the earlier iterations of the process.

III. GEOLOGY OF THE REGION

The study area is located in the Fars province, approximately 180 kilometers southeast of Shiraz, in the Fasa county, specifically in the Sheshdeh section. This area is situated within the folded zone of the Zagros geological belt. The Zagros zone is part of the folded region in southwestern Iran and is bounded to the east by the Minab fault. Its geological structure is simple, consisting of a series of closely spaced, compressed anticlines with generally vertical axial planes and a NW to SE orientation. The majority of the folded sediments in this region are composed of limestone with dolomite, accompanied by marl and marly limestone, characterized by relatively fine stratification. The folded Zagros region, from the Upper Triassic period onward, has had a geological history distinct from other parts of Iran, forming a basin with continuous subsidence and ongoing sedimentation (Yousefi and Andalibi, 2002).

In Fig. 3, two active working places are illustrated: one located at the summit of the mountain (a) and the other positioned at its base (b). Notably, this fracturing diminishes as one delves deeper into the mountain's structure. The extent of fragmentation observed at the upper section of the mountain is pronounced enough to

have led to the creation of a macadam layer composed of marble, which unfortunately fails to meet the essential quality standards necessary for extraction purposes.

Main units in the studied area are the Asmari and Jahrom formations (PEMj-as). The two geological formations are intricately linked, comprising medium to thick layers of fossil-rich limestones and dolomitic limestones, with the lower section often featuring marl-limestone primarily associated with the Jahrom Formation. In contrast, the upper section showcases less weathered limestones characterized by distinct bedding, interspersed with thin layers of marl, predominantly linked to the Asmari Formation. This remarkable formation dates back to the Eocene-Oligocene epoch, highlighting its significant geological history.

Quaternary deposits (*Qc*) are characterized by their coarse conglomerate structure, exhibiting a moderate degree of hardness. Within these deposits, one can find a diverse array of well-rounded fragments, predominantly gravel-sized, which reflect the geological characteristics of the adjacent hills. Notably, these conglomerate formations overlay the remnants of ancient alluvial plains, creating a fascinating interplay between past and present geological processes(Yousefi and Andalibi, 2002).

In contrast, the Qap deposits are situated within dynamic floodplain environments, riverbeds, and watercourses, where they primarily consist of sandy, gravelly, and pebble-sized sediments. These accumulations are not merely relics of the past; they continue to evolve and form in response to the ongoing natural processes occurring in these vibrant ecosystems. A comprehensive geological map of the region, prepared at a scale of 1:10000, is presented in Fig. 4, which also highlights the positions of the three survey profiles. All three profiles are in the PEMj-as unit.

IV. GEOELECTRICAL MODELING

Utilizing the measured field data, which encompasses both geophysical and surface geological insights, initial pseudo-sections are plotted for each profile. These representations feature pseudo-sections that illustrate electrical resistivity and induced polarization. Throughout the modeling phase, the elevations of the electrode stations along the profiles are instrumental in implementing topographic corrections. This entails a careful calculation and application of the influence that topography exerts on the positioning and intensity of the measured parameters, ensuring a refined and accurate interpretation of the data. The 2D models developed along the profile length, and the z-axis, indicating elevation above sea level, offer valuable insights into the trajectory of the profile. To analyze the resistivity (RS) and induced polarization (IP) data, inverse modeling is conducted utilizing a structured mesh through the "Res2Dinv" software.

Fig. 3. Morphological status of the Fasa marble area with a layer of sandstone and debris (a) active working location, (b) old working location

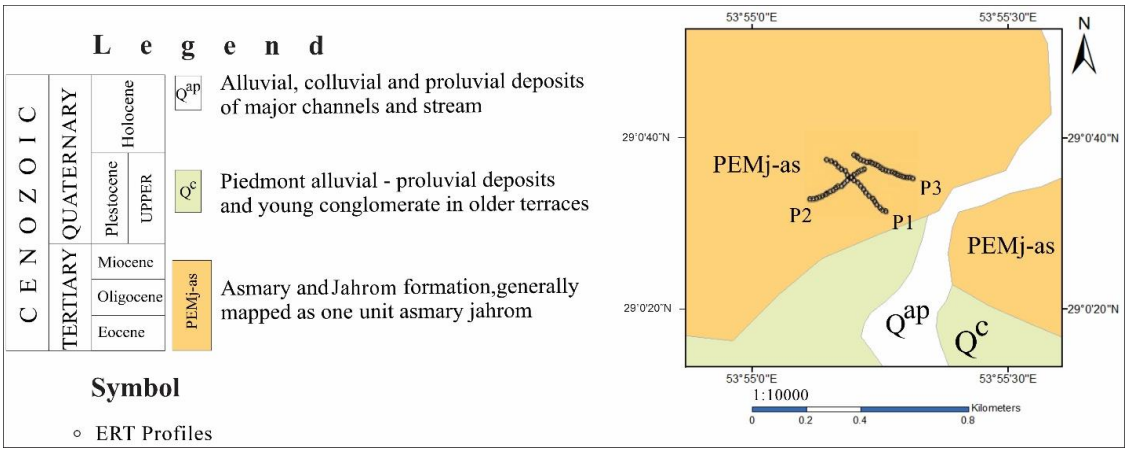

Fig. 4. Geological map of the study area, and the location of three geoelectrical profiles

The study's results encompass three distinct ERT lines. The survey employed a variety of configurations, integrating both dipole-dipole and pole-dipole array setups, with electrode spacings set at 15 meters and 10 meters. Throughout the three profiles examined in the study area, a comprehensive total of 1,000 readings for both IP and RS data were accurately recorded. In the execution of the dipole-dipole and pole-dipole arrays, depth measurements were systematically read up to ten times of electrode separation, ensuring a thorough exploration of the subsurface characteristics and successfully exploring a depth of approximately 70 meters across the designated profiles.

Three profiles were surveyed, such that two profiles with an approximate NW-SE orientation (Profiles 1 and 3) and one profile with a NE-SW orientation (Profile 2) measured time domain data. The inversion algorithm was designed to terminate at an iteration where the RMS error approximates 2. This threshold was selected in consideration of the significant noise present in the observed ERT data. Following the careful input of data and the execution of 14 to 16 iterative inversions, the resultant model data demonstrated an optimal correlation with the observed data, as illustrated in Fig.s 5 and 6. In this modeling endeavor, the subsurface physical model was meshed utilizing a 15-meter electrode spacing for Profiles 1, while Profiles 2 and 3 were configured with a more refined 10-meter electrode spacing. The resulting mesh blocks were designed to be 7.5 meters and 10 meters in size, respectively, ensuring a detailed representation of the subsurface features. Furthermore, the geological sections corresponding to each survey line can be discerned from the variations in electrical resistivity and induced polarization values obtained through data inversion, as illustrated in Figs. 7, 8, and 9.

Given the dominant horizontal layering and stratigraphic structure of the marble building stone in the study area, the inversion algorithm prioritized enhancing the horizontal weighting (horizontal flatness) during the reconstruction of electrical resistivity models. This approach was adopted to ensure alignment between the derived geophysical results and the region's established geological framework

V. GEOLOGICAL INTERPRETATION

The findings derived from the numerical modeling, alongside the electrical resistivity and induced polarization data across the three geoelectrical profiles, reveal a distinct boundary delineating the sandstone and limestone layer from the underlying strata characterized by lower electrical resistivity. This boundary exhibits a thickness that fluctuates between 0 and a maximum of 30 meters. Furthermore, the electrical model indicates that the marble layer possesses a thickness ranging from 10 to 30 meters, distinguished by its elevated electrical resistivity values. It is particularly noteworthy that these two geological layers are distinctly separated, a consequence of their marked disparity in electrical resistivity. Additionally, the induced polarization models indicate that with a modest increase in polarization values, the limestone and marl bed, which contains marble, becomes increasingly pronounced at depths extending from 30 to 40 meters.

The physical and mechanical integrity of marble stones is significantly influenced by the presence of fractures, cracks, and breaks within their structure. Generally speaking, a reduction in these discontinuities correlates with an increase in the rock's density, which in turn enhances its electrical resistivity. Geological studies and empirical data indicate that the finest quality marble specimens are predominantly located on the southern slope of the region. This phenomenon can be attributed to unique geological conditions, tectonic activities, and the specific processes that shaped these rocks in that locale. Conversely, in certain areas, particularly those characterized by a macadamized surface, one may encounter lower-quality stones that exhibit a greater prevalence of fractures and cracks. Such imperfections lead to diminished density and resistivity, underscoring the importance of geological context in assessing marble quality.

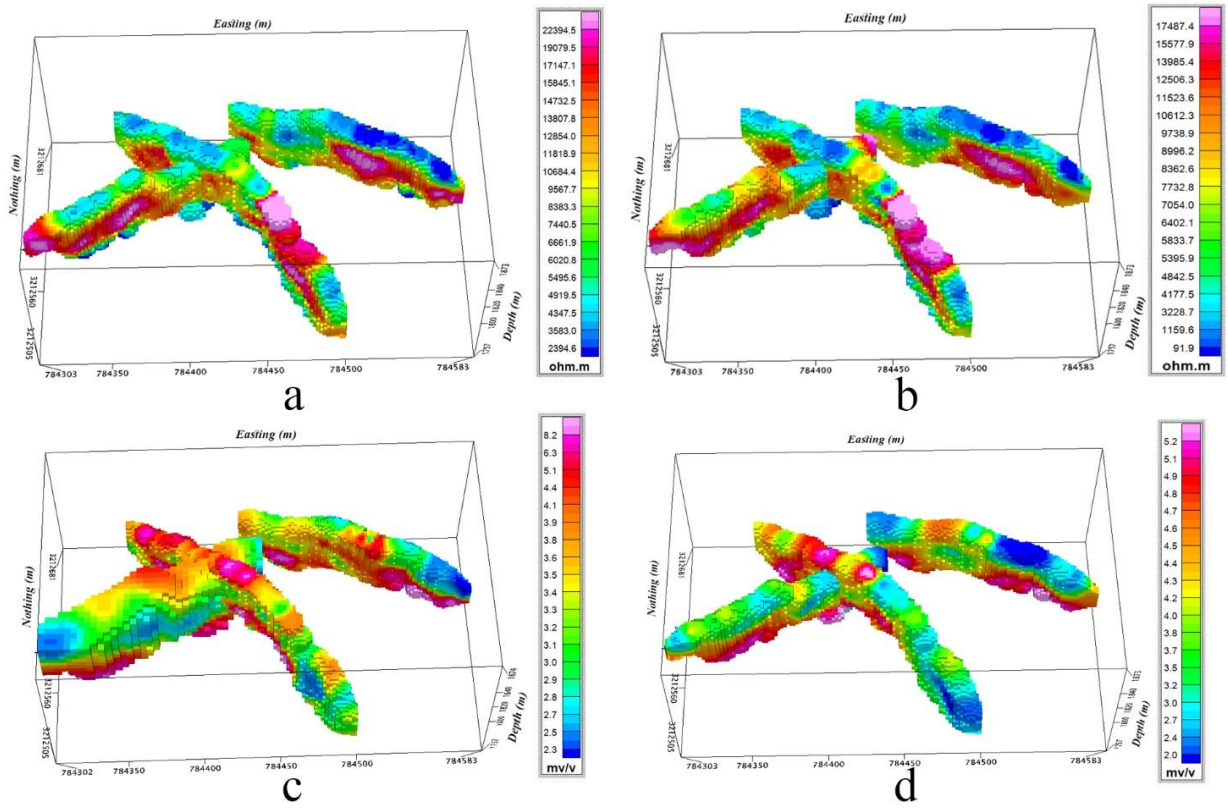

Fig. 5. 3D display of observed apparent electrical resistivity (a), observed apparent chargeability (b), predicted electrical resistivity (c), and predicted chargeability (d) from 2D inverse modeling.

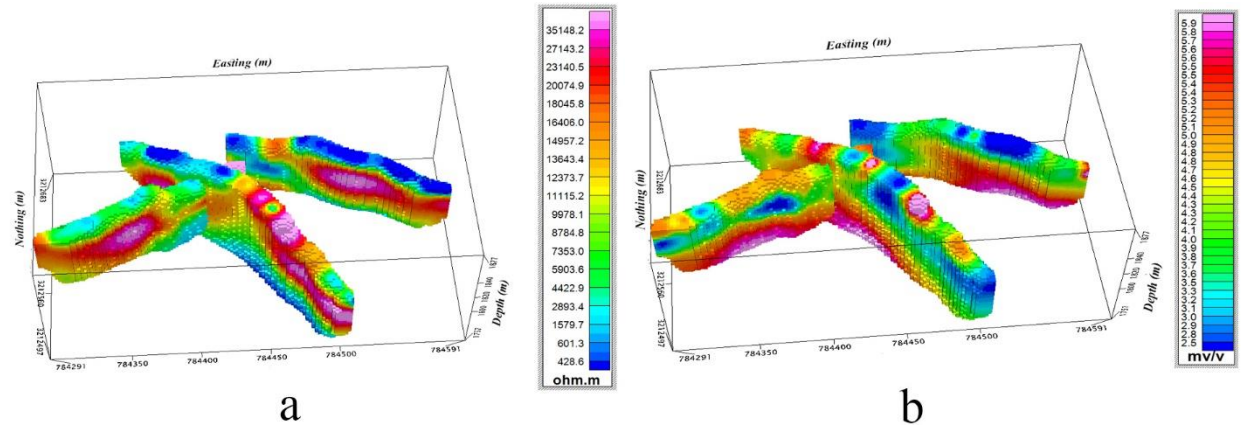

Fig. 6. Inversion result of geoelectrical data: (a) electrical resistivity model and (b) chargeability model

In order to attain a more precise evaluation of the marble quality found on the southern slope and to effectively differentiate it from samples located in the macadamized regions, the implementation of multiple exploratory boreholes is deemed crucial. These boreholes will facilitate a thorough investigation into the internal composition, density, and fracture distribution of the rock, thereby enabling a definitive assessment of its overall quality. While no laboratory analyses have been conducted on core samples from the study area, field observations indicate distinct geoelectrical properties between lithologies. High-quality, intact marble units exhibit significantly elevated resistivity and reduced chargeability compared to limestone/marl formations (Fig. 3b). In folded marble sequences, zones of intense folding are particularly susceptible to fracturing from lateral stress. Such fracturing (macadamization) enhances secondary porosity, potentially facilitating fluid retention (Fig. 3a). This hydrogeological modification would manifest as decreased resistivity and degraded stone quality in geophysical surveys.

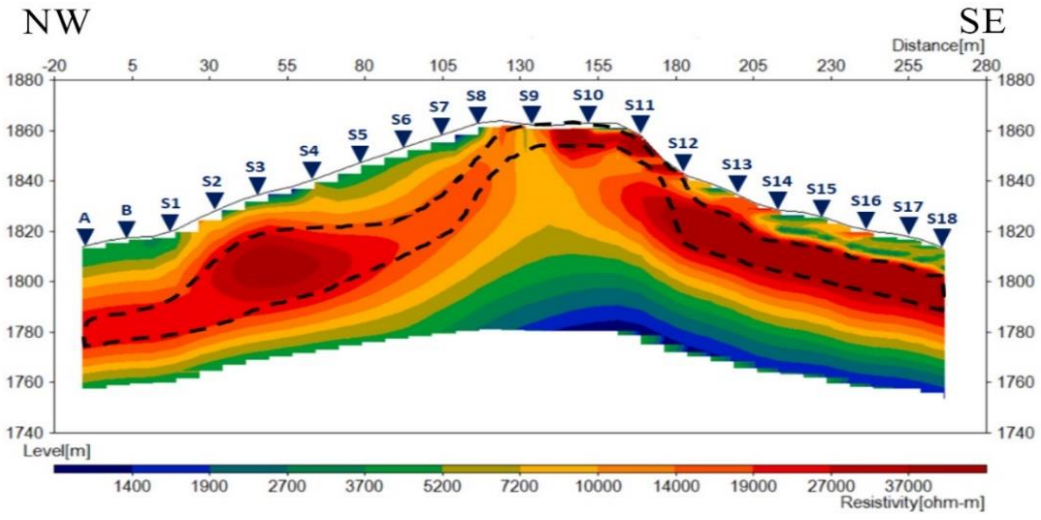

(a)

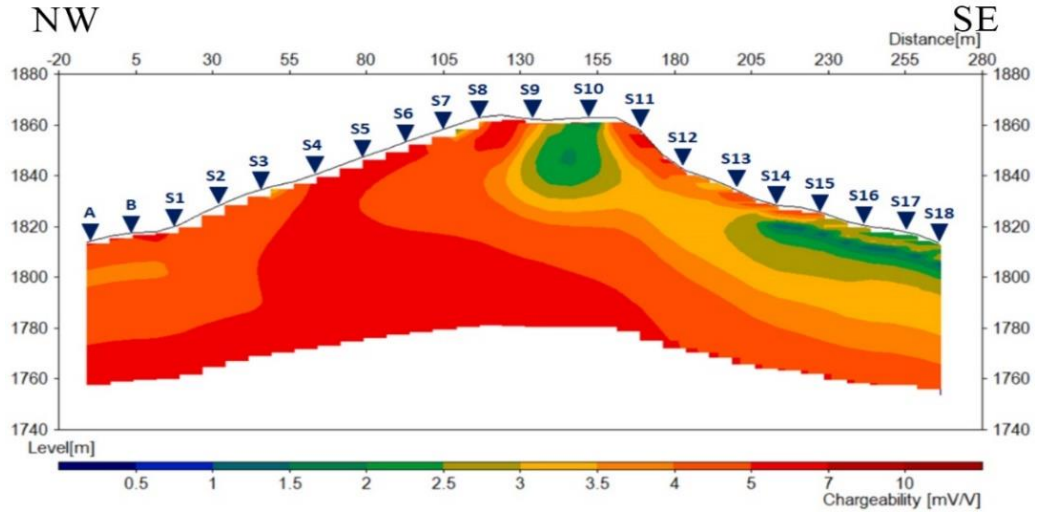

(b)

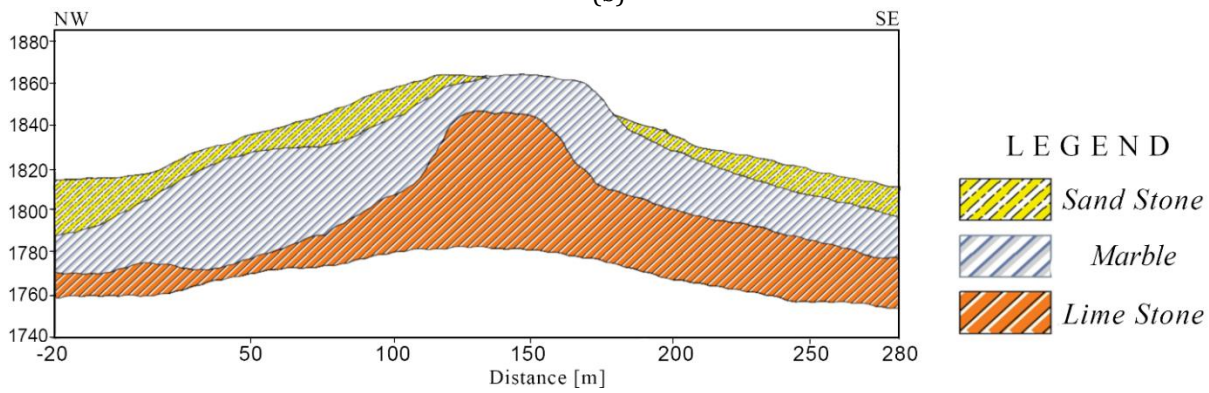

(c)

Fig. 7. Models of electrical resistivity (a), chargeability (b), and plausible geological map (c) along the ERT profile 1. The marble stratification exhibits notably higher electrical resistivity compared to the surrounding limestone/marl substrate, whereas its differentiation is further accentuated by significantly lower electrical chargeability.

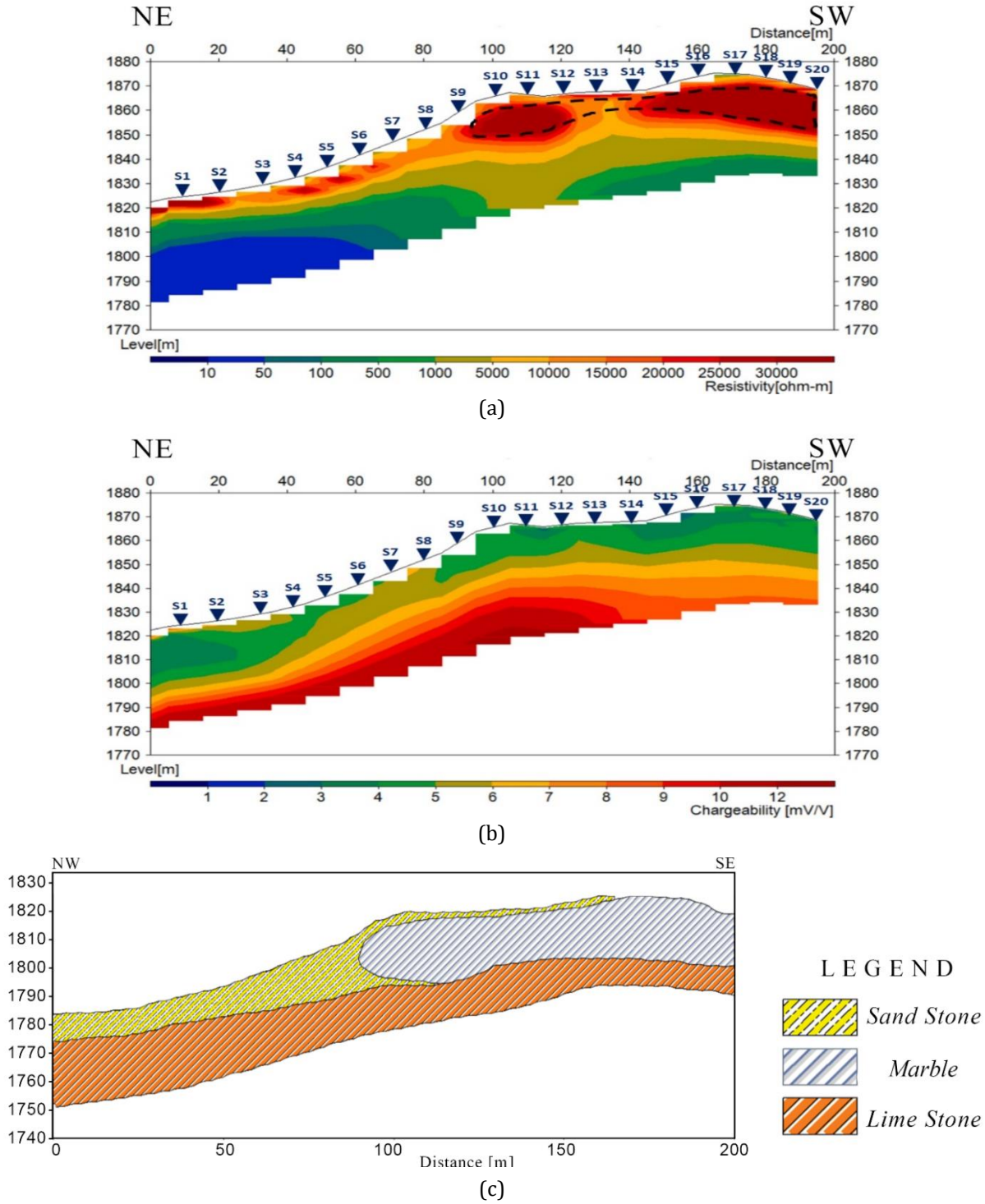

Fig. 8. Models of electrical resistivity (a), chargeability (b), and plausible geological map (c) along the ERT profile 2. The marble stratification exhibits notably higher electrical resistivity compared to the surrounding limestone/marl substrate, whereas its differentiation is further accentuated by significantly lower electrical chargeability.

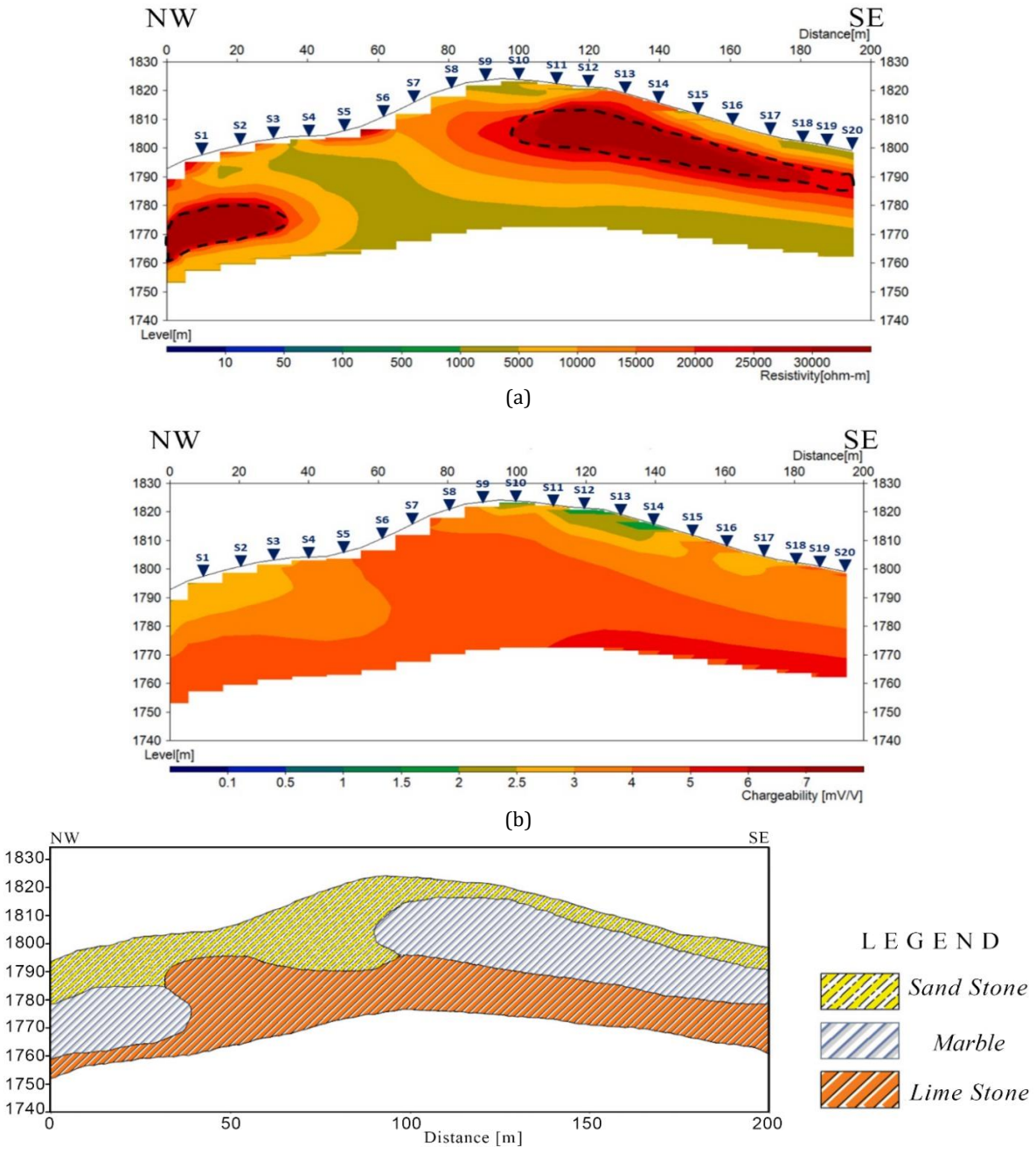

Fig. 9. Models of electrical resistivity (a), chargeability (b), and plausible geological map (c) along the ERT profile 3. The marble stratification exhibits notably higher electrical resistivity compared to the surrounding limestone/marl substrate, whereas its differentiation is further accentuated by significantly lower electrical chargeability.

VI. CONCLUSION

This research endeavor sought to uncover geological formations and marble building stones at the Sheshdeh mine located in Fasa, Iran, with the overarching aim of assessing marble reserves. To achieve this, numerical modeling of geoelectric data was executed utilizing a structural mesh framework. The findings presented in this study stem from electrical investigations conducted along three designed profiles. The geoelectric data encompasses electrical resistivity and induced polarization values pertinent to these profiles. The primary objective of this investigation was to delineate the positioning of marble layers while examining their geometry, depth, and quality, particularly concerning fractures and fissures. Subsequently, leveraging the available technological tools, an inversion process was carried out to thoroughly evaluate the potential for extracting valuable information from the data collected.

Three geoelectrical profiles exhibiting elevated electrical resistivity values have effectively delineated the marble stone from the adjacent geological materials. According to the electrical model, the marble layer's thickness ranges from 10 to 30 meters, while the overlying sandstone and limestone layer displays

thickness variations from negligible to a maximum of 30 meters, characterized by its comparatively lower electrical resistivity. Chargeability models reveal a subtle increase in chargeability values at depths between 30 and 40 meters, indicating the presence of a limestone/marl bed that underlies the marble. The findings from the electrical resistivity models suggest that the marble located on the southern slope possesses superior quality compared to that found along the mountain's ridge line. The denser and less fractured the marble stone is, the higher its electrical resistivity, leading to the conclusion that the southern slope harbors marble of enhanced quality. To accurately assess the quality of the marble and to distinguish it from weathered regions, there is an immediate necessity to conduct several exploratory boreholes in the southern slope.

ACKNOWLEDGMENTS

The authors wish to extend their heartfelt thanks and deep appreciation to the Faculty of Mining Engineering at the College of Engineering, University of Tehran, for generously supplying the data that formed the foundation of this study.

REFERENCES

Abedi, M., & Afshar, A. (2022). Geoelectrical studies using IP & RS method in the Sheshdeh marble area, Fasa, Technical Report, Razian Marmarit Tous Company.

Ahmed, W., Ahmad, N., Janjuhah, H. T., Islam, I., Sajid, M., & Kontakiotis, G. (2023). The evaluation of non-destructive tests for the strength and physical properties of granite, marble, and sandstone: a case study from North Pakistan. Quaternary, 6(1), 4.

Annan, P. (2003). Ground penetrating radar principles, procedures and applications. Sensors and software, 278.

Annan, A. P., & Jol, H. M. (2009). Ground penetrating radar: Theory and applications. Electromagnetic principles of ground penetrating radar, 3-40.

Binley, A., & Kemna, A. (2005). DC resistivity and induced polarization methods. In Hydrogeophysics (pp. 129-156). Dordrecht: Springer Netherlands.

Cardarelli, E., Cercato, M., Cerreto, A., & Di Filippo, G. (2010). Electrical resistivity and seismic refraction tomography to detect buried cavities. Geophysical prospecting, 58(4), 685-695.

Cardarelli, E., & Fischanger, F. (2006). 2D data modelling by electrical resistivity tomography for complex subsurface geology. Geophysical Prospecting, 54(2), 121-133.

Constable, S. C., Parker, R. L., & Constable, C. G. (1987). Occam's inversion: A practical algorithm for generating smooth models from electromagnetic sounding data. Geophysics, 52(3), 289-300.

Dahlin, T. (1996). 2-D resistivity surveying for engineering and environmental applications. First Break, 14(7), 275-283.

Darvill, T., Lüth, F., Rassmann, K., Fischer, A., & Winkelmann, K. (2013). Stonehenge, Wiltshire, UK: high resolution geophysical surveys in the surrounding landscape, 2011. European Journal of Archaeology, 16(1), 63-93.

Demirel, S., Roubinet, D., Irving, J., & Voytek, E. (2018). Characterizing near-surface fractured-rock aquifers: insights provided by the numerical analysis of electrical resistivity experiments. Water, 10(9), 1117.

Dentith, M., & Mudge, S. T. (2014). Geophysics for the mineral exploration geoscientist. Cambridge University Press.

Dey, A., & Morrison, H. F. (1979). Resistivity modelling for arbitrarily shaped two-dimensional structures. Geophysical prospecting, 27(1), 106-136.

Edigbue, P. I., Al-Mashhor, A. A., Plougarlis, A., Soupios, P., Tranos, M., Kaka, S., ... & Al-Garni, M. (2021). Geological and geophysical investigations of an engineering site characterization for construction purposes in Western Saudi Arabia. Journal of Applied Geophysics, 188, 104307.

Ganiyu, S. A., Oladunjoye, M. A., Onakoya, O. I., Olutoki, J. O., & Badmus, B. S. (2020). Combined electrical resistivity imaging and ground penetrating radar study for detection of buried utilities in Federal University of Agriculture, Abeokuta, Nigeria. Environmental Earth Sciences, 79, 1-20.

Hoover, D. B., Klein, D. P., Campbell, D. C., & du Bray, E. (1995). Geophysical methods in exploration and mineral environmental investigations. Preliminary compilation of descriptive geoenvironmental mineral deposit models: USGS Open-File Report, 95(831), 19-27.

Jarzyna, J. A., Dec, J., Karczewski, J., Porzucek, S., Tomecka-Suchoń, S., Wojas, A., & Ziętek, J. (2012). Geophysics in near-surface investigations. New achievements in geoscience, 46-80.

Keller, G. V., & Frischknecht, F. C. (1966). Electrical methods in geophysical prospecting.

Kemna, A., Binley, A., Ramirez, A., & Daily, W. (2000). Complex resistivity tomography for environmental applications. Chemical Engineering Journal, 77(1-2), 11-18.

Loke, M. H., & Barker, R. D. (1996). Rapid Least-Squares Inversion of Apparent Resistivity Pseudosections by a Quasi-Newton Method. Geophysical Prospecting, 44(1), 131-152.

Loke, M. H., Dahlin, T., & Rucker, D. F. (2014). Smoothness-constrained time-lapse inversion of data from 3D resistivity surveys. Near surface geophysics, 12(1), 5-24.

Loke, M. H. (2018). Tutorial notes on 2D Electrical Imaging Surveys.

Martinez, J., Montiel, V., Rey, J., Canadas, F., & Vera, P. (2017). Utilization of integrated geophysical techniques to delineate the extraction of mining bench of ornamental rocks (marble). Remote Sensing, 9(12), 1322.

Oldenburg, D. W., & Li, Y. (1999). Estimating Depth of Investigation in DC Resistivity and IP Surveys. Geophysical Journal International, 137(3), 605-617.

Olona, J., Pulgar, J. A., Fernández-Viejo, G., López-Fernández, C., & González-Cortina, J. M. (2010). Weathering variations in a granitic massif and related geotechnical properties through seismic and electrical resistivity methods. Near Surface Geophysics, 8(6), 585-599.

Reynolds, J. M. (2011). An introduction to applied and environmental geophysics. John Wiley & Sons.

Rücker, C., Günther, T., & Spitzer, K. (2006). Three-dimensional modelling and inversion of dc resistivity data incorporating topography—I. Modelling. Geophysical Journal International, 166(2), 495-505.

Sharma, S., & Verma, G. K. (2015). Inversion of electrical resistivity data: a review. International Journal of Computer and Systems Engineering, 9(4), 400-406.

Sumner, J. S. (2012). Principles of induced polarization for geophysical exploration. Elsevier.

Talebi, M.A., Abedi, M., Moradzadeh, A., & Afshar, A. (2022a). Geophysical modeling of electrical resistivity and induced polarization data for exploration of building stones: A case study - Atashkooh travertine. JOURNAL OF RESEARCH ON APPLIED GEOPHYSICS, 8 (1), 27-40.

Talebi, M.A., Abedi, M., & Moradzadeh, A. (2022b). Geoelectrical modeling of travertine rocks beneath a rough topographical relief using structured and unstructured meshes. Acta Geodaetica et Geophysica, 57, 351–372.

Telford, W. M., Geldart, L. P., & Sheriff, R. E. (1990). Applied geophysics. Cambridge university press.

Uhlemann, S., Chambers, J., Falck, W. E., Tirado Alonso, A., Fernández González, J. L., & Espín de Gea, A. (2018). Applying electrical resistivity tomography in ornamental stone mining: Challenges and solutions. Minerals, 8(11), 491.

Yousefi, T., & Andalibi, M.J. (2002).Geological sheet 1:100,000 Runiz